



Development of Lee's exact method for Gauss–Krüger projection

Jia-Chun Guo^{1,2} · Wen-Bin Shen^{1,2} · Jin-Sheng Ning^{1,2}

Received: 17 August 2019 / Accepted: 4 June 2020 / Published online: 23 June 2020
© Springer-Verlag GmbH Germany, part of Springer Nature 2020

Abstract

Lee's exact method was developed to enable the Gauss–Krüger (GK) projection to be implemented without iterative procedures via the expansion of the intermediate mapping (Thompson projection) into series approximations in terms of isothermal coordinates (ψ, λ) for the forward mapping and GK coordinates (x, y) for the reverse mapping. The straightforward procedures expressed by new formulas for both forward and reverse mapping of the GK projection were composed by three sequential steps which essentially reveal the mapping procedures and intrinsic properties of the GK projection: The first step of deriving the isothermal coordinates (ψ, λ) from the geodetic coordinates (φ, λ) specifies a conformal mapping (i.e., the Normal Mercator projection) of the Earth ellipsoid surface into the Euclidean plane excluding the South and North poles, and the subsequent two steps allow the GK projection to be expressed analytically via the elliptic functions and integrals. Based on the three-step procedure, the conformality and singularities over the entire ellipsoid of the Normal Mercator, Thompson and GK projections were analyzed and the fundamental domains of them were determined. With respect to the precision and efficiency, it was verified that the new algorithm and the complex latitude method had equivalent precision levels for the same orders of the third flattening n with the Krüger- n series from n^2 to n^{12} but slower about 0.19 to 0.21 μs than the Krüger- n series for a GK coordinates calculating. However, the new formulas provide series approximations for the forward mapping of the Thompson projection and projective transformations for the Normal Mercator, Thompson and GK projections.

Keywords Geometrical Geodesy · Map projections · Conformal mapping · Elliptic functions and integrals

1 Introduction

The Gauss–Krüger projection or Transverse Mercator (abbreviated as GK hereinafter) is widely applied in the geodetic community for accurate geodetic measurements and large-scale maps of zones due to its excellent qualities, especially its conformality and high accuracy. Generally, the GK projection can be expressed in an ellipsoidal or spherical version depending on the type of mathematical reference surface, ellipsoid or sphere, that is chosen to model the Earth. In this study, the reference surface is always assumed to be an oblate ellipsoid of revolution.

Assuming the central meridian to be selected at the origin of the longitudes and the scale of it to be unity, the standard form of the GK projection can be defined by the complex-valued function (e.g., Thompson 1975)

$$z = x + iy = S(\chi) = \int_0^{\chi=\psi+i\lambda} r(\chi) d\chi \quad (1)$$

with the initial value

$$z|_{\lambda=0} = S(\psi) = \int_0^{\psi} r(\psi) d\psi \quad (2)$$

on the central meridian, where the imaginary unit and complex variables are denoted in lowercase italic boldface (similarly hereinafter):

- imaginary unit i is defined by $i^2 = -1$;
- $z = x + iy$ represents the complex GK coordinate, with the real part x for northing and the imaginary part y for easting;
- $\chi = \psi + i\lambda$ denotes the complex isometric latitude, in which the isometric latitude ψ is defined as the real

✉ Wen-Bin Shen
wbshen@sgg.whu.edu.cn

Jia-Chun Guo
jchguo@whu.edu.cn

¹ School of Geodesy and Geomatics, Wuhan University, Wuhan, China

² Key Laboratory of Geospace Environment and Geodesy, Ministry of Education, Wuhan, China

part, and the longitude λ is defined as the imaginary part (mathematically, (ψ, λ) is called isothermal coordinates, see Sect. 5);

- $S(\psi)$ represents the meridian arc length between the equator and the parallel ψ , and $r(\psi)$ is the radius of the parallel in terms of isometric latitude ψ (Bermejo-Solera and Otero 2009 Eqs. (1) and (9)).

In general, the isometric latitude ψ of a given point on the ellipsoid at geodetic latitude φ is computed by (e.g., Hotine 1946; Lambert 1972)

$$\psi = \psi(\varphi) = \int_0^\varphi \frac{1 - e^2}{(1 - e^2 \sin^2 \varphi) \cos \varphi} d\varphi \tag{3}$$

$$= \operatorname{arctanh}(\sin \varphi) - e \operatorname{arctanh}(e \sin \varphi),$$

where e denotes the first eccentricity of the ellipsoid.

From the perspective of complex analysis (e.g., McConnell 2013), the GK projection is conformal if and only if the function defined by Eq. (1) is biholomorphic (bijective and holomorphic) on an open, connected and non-empty set (for a detailed discussion about the domain and property of the projection, see Sect. 5). Let $x = x(\psi, \lambda)$ and $y = y(\psi, \lambda)$, conformality of the GK projection implies that (1) the partial derivatives of x and y must exist and satisfy the Cauchy–Riemann equations

$$\begin{cases} \frac{\partial x}{\partial \psi} = \frac{\partial y}{\partial \lambda} \\ \frac{\partial x}{\partial \lambda} = -\frac{\partial y}{\partial \psi}, \end{cases} \tag{4}$$

and (1) the function is bijective (one-to-one correspondence) and the derivative of $S(\chi)$ has four equivalent forms and is everywhere nonzero on the domain:

$$\begin{aligned} S'(\chi) &= \frac{dz}{d\chi} = r(\chi) \\ &= \frac{\partial x}{\partial \psi} + i \frac{\partial y}{\partial \psi} = \frac{\partial y}{\partial \lambda} - i \frac{\partial x}{\partial \lambda} \\ &= \frac{\partial x}{\partial \psi} - i \frac{\partial x}{\partial \lambda} = \frac{\partial y}{\partial \lambda} + i \frac{\partial y}{\partial \psi} \neq 0. \end{aligned} \tag{5}$$

Equations (1) to (3) give a neat definition of the GK projection, and Eqs. (4) and (5) provide the necessary and sufficient conditions for the mapping to be conformal. This projection seems simple but is actually complex since the integrand $r(\chi)$ in Eq. (1) is inexpressible in closed form by any known function of χ .

Based on this definition, various methods have been developed over the past century for computing the mapping, and most of these methods are based on power series, e.g., the “Krüger- λ ” and “Krüger- n ” series (in terms of difference of longitude λ and the third flattening n , respectively)

established by Krüger (1912) and developed by many others geodesists (e.g., Redfearn 1948; König and Weise 1951; Thomas 1952; Enríquez 2004; Engsager and Poder 2007; Turiúo 2008; Karney 2011), the bivariate series around a selected point (φ_0, λ_0) provided by Grafarend and Syffus (1998) and the perturbation series in terms of the complex isometric latitude χ constructed by Bermejo-Solera and Otero (2009).

On the other hand, if normally expressing the meridian arc length in terms of geodetic latitude φ as

$$S(\psi) = m(\varphi) = \int_0^\varphi \frac{a(1 - e^2)}{(1 - e^2 \sin^2 \varphi)^{3/2}} d\varphi \tag{6}$$

and expanding the geodetic latitude φ to the complex one, denoted by φ_c , then, as described by Poder and Engsager (1998), the GK projection is defined by

$$z = x + iy = \int_0^{\varphi_c} \frac{a(1 - e^2)}{(1 - e^2 \sin^2 \varphi_c)^{3/2}} d\varphi_c \tag{7}$$

and

$$\chi = \psi + i\lambda = \operatorname{arctanh}(\sin \varphi_c) - e \operatorname{arctanh}(e \sin \varphi_c), \tag{8}$$

where a is the semimajor axis the ellipsoid. Similar to $r(\chi)$, the complex latitude φ_c is also inexpressible in closed form by means of any known functions.

With this definition, series expansion for the complex GK coordinate $z = x + iy$ was expanded to n^7 by Engsager and Poder (2007).

Among these various methods derived from the above two definitions, the most commonly used methods are the “Krüger- λ ” and “Krüger- n ” series. The “Krüger- λ ” series were the first to be implemented on the hand calculators of the mid-twentieth century but were verified not to be accurate enough for wide-zone use, e.g., for mapping Greenland in one zone (Karney 2011). Correspondingly, the extending “Krüger- n ” series were recommended for implementing the GK projection (e.g., Engsager and Poder 2007; Karney 2011; PROJ contributors 2020).

However, theoretically, the characterization of both the local and global features of the GK projection cannot be accomplished competently by only the above two definitions or any series expansion methods since $r(\chi)$ and φ_c are inexpressible in closed form by any known function.

In particular, besides the above two definitions, Lee (1962, 1963, 1976) explored a new avenue to express the GK projection by using elliptic functions and integrals. Tracing to its origin, similar formulations were also independently provided by Ludwig (1943). Lee’s formulas give analytical functions for the forward solution of the GK projection and thus is generally named Lee’s exact method. It will be

shown by our analyses that Lee’s exact method is considered important for a deep insight of the GK projection, especially for the entire property. However, unfortunately, the method is not commonly used in practice and even seems to be falling into obscurity in the geodetic community (Dorrer 2003).

Considering the merits of Lee’s method for analytical investigation of the properties of the GK projection, in this study, we developed straightforward procedures for both the forward and inverse mapping of the GK projection via Lee’s exact method and, based on this, the entire properties and the fundamental domains of the three projections, Normal Mercator, Thompson and GK, were analyzed and determined.

2 Forward mapping by Lee’s exact method without iteration

2.1 Review of Lee’s exact method

Essentially, the meridian is related to the elliptic integral of the second kind (e.g., Ludwig 1943; Dozier 1980; Dorrer 2003). Omitting the derivation procedure, we show the formulas directly as

$$\begin{aligned}
 m(\varphi) &= a E(\varphi, e) - \frac{a e^2 \sin \varphi \cos \varphi}{\sqrt{1 - e^2 \sin^2 \varphi}} \\
 &= a E(u) - \frac{a e^2 \operatorname{sn} u \operatorname{cn} u}{\operatorname{dn} u} \\
 &= a E(K + u) - a E,
 \end{aligned} \tag{9}$$

where

$$\begin{cases}
 u = F(\varphi, e) = \int_0^\varphi \frac{1}{\sqrt{1 - e^2 \sin^2 \varphi}} d\varphi \\
 E(\varphi, e) = \int_0^\varphi \sqrt{1 - e^2 \sin^2 \varphi} d\varphi \\
 E(\varphi, e) = E(u) = \int_0^u \operatorname{dn}^2 u du
 \end{cases} \tag{10}$$

represent the incomplete elliptic integrals of the first and second kinds with the elliptic modulus e , respectively, and correspondingly, $K = F(\pi/2, e)$ and $E = E(\pi/2, e)$ represent the complete integrals of the first and second kinds (note that, following mathematical convention, E represents a constant but not a function when is solely used, e.g., Byrd and Friedman 1971 §110); the principal Jacobian sine, cosine and delta elliptic functions with the elliptic modulus e are defined by

$$\begin{cases}
 \operatorname{sn} u = \operatorname{sn}(u, e) = \sin \varphi \\
 \operatorname{cn} u = \operatorname{cn}(u, e) = \cos \varphi \\
 \operatorname{dn} u = \operatorname{dn}(u, e) = \sqrt{1 - e^2 \sin^2 \varphi}.
 \end{cases} \tag{11}$$

Also in terms of Jacobian function, the isometric latitude ψ defined in Eq. (3) can be rewritten as:

$$\psi = \operatorname{arctanh}(\operatorname{sn} u) - e \operatorname{arctanh}(e \operatorname{sn} u). \tag{12}$$

If the incomplete elliptic integral of the first kind u is extended to the complex plane as $w = u + iv$ and substituted into Eq. (9), then the GK projection defined by Eqs. (1) to (3) can be also defined by

$$\begin{aligned}
 z = f(w) &= a E(w) - \frac{a e^2 \operatorname{sn} w \operatorname{cn} w}{\operatorname{dn} w} \\
 &= a E(K + w) - a E
 \end{aligned} \tag{13}$$

and

$$\chi = \operatorname{arctanh}(\operatorname{sn} w) - e \operatorname{arctanh}(e \operatorname{sn} w), \tag{14}$$

where u and v , the real and imaginary parts of w are redefined by amplitudes α and β , respectively (Ludwig 1943 Eqs. (60) and (61)):

$$\begin{cases}
 u = F(\alpha, e) = \int_0^\alpha \frac{1}{\sqrt{1 - e^2 \sin^2 \alpha}} d\alpha \\
 v = F(\beta, \sqrt{1 - e^2}) = \int_0^\beta \frac{1}{\sqrt{1 - (1 - e^2) \sin^2 \beta}} d\beta.
 \end{cases} \tag{15}$$

The projection defined by the inverse of Eq. (14) is known as the Thompson projection that was established but not published by himself in 1945 and subsequently developed by Lee (1962, 1963). Note that, however, similar formulations were independently provided by Ludwig (1943).

Separating the real and the imaginary parts of Eqs. (13) and (14) gives (for more details, see Lee 1962)

$$\begin{cases}
 x = a E(u) - \frac{a e^2 \operatorname{sn} u \operatorname{cn} u \operatorname{dn} u}{\operatorname{dn}^2 u + \operatorname{dn}'^2 v - 1} \\
 y = a v - a E'(v) + \frac{a(1 - e^2) \operatorname{sn}' v \operatorname{cn}' v \operatorname{dn}' v}{\operatorname{dn}^2 u + \operatorname{dn}'^2 v - 1}
 \end{cases} \tag{16}$$

and

$$\begin{cases}
 \psi = \operatorname{arctanh}(\operatorname{sn} u \operatorname{dn}' v) - e \operatorname{arctanh}(e \operatorname{sn} u \operatorname{nd}' v) \\
 \lambda = \operatorname{arctan}(\operatorname{dc} u \operatorname{sc}' v) - e \operatorname{arctan}(e \operatorname{cd} u \operatorname{sc}' v),
 \end{cases} \tag{17}$$

where any one of the elliptic functions and integrals with or without “'” corresponds to its elliptic modulus $\sqrt{1 - e^2}$ or e , respectively, e.g., $\operatorname{sn}' v = \operatorname{sn}(v, \sqrt{1 - e^2})$ and $\operatorname{sn} u = \operatorname{sn}(u, e)$; the subsidiary Jacobian elliptic functions are denoted following the Glaisher’s Notation (e.g., Olver et al.

2010 §22.2): let p, q, r be any three of the letters s, c, d, n , then

$$p \ q(u, e) = \frac{p \ r(u, e)}{q \ r(u, e)} = \frac{1}{q \ p(u, e)}, \tag{18}$$

e.g., $dc \ u = dn \ u / cn \ u = 1 / cd \ u$.

Alternatively, using the definitions of u and v in Eqs. (15), (16) and (17) can be rewritten in terms of (α, β) as

$$\begin{cases} x = a E(\alpha, e) - \frac{a e^2 \sin \alpha \cos \alpha \sqrt{1 - e^2 \sin^2 \alpha}}{1 - e^2 \sin^2 \alpha - (1 - e^2) \sin^2 \beta} \\ y = a F(\beta, \sqrt{1 - e^2}) - a E(\beta, \sqrt{1 - e^2}) \\ \quad + \frac{a(1 - e^2) \sin \beta \cos \beta \sqrt{1 - (1 - e^2) \sin^2 \beta}}{1 - e^2 \sin^2 \alpha - (1 - e^2) \sin^2 \beta} \end{cases} \tag{19}$$

and

$$\begin{cases} \psi = \operatorname{arctanh} \left(\sin \alpha \sqrt{1 - (1 - e^2) \sin^2 \beta} \right) \\ \quad - e \operatorname{arctanh} \left(\frac{e \sin \alpha}{\sqrt{1 - (1 - e^2) \sin^2 \beta}} \right) \\ \lambda = \operatorname{arctan} \left(\tan \beta \sqrt{\sec^2 \alpha - e^2 \tan^2 \alpha} \right) \\ \quad - e \operatorname{arctan} \left(\frac{e \tan \beta}{\sqrt{\sec^2 \alpha - e^2 \tan^2 \alpha}} \right), \end{cases} \tag{20}$$

respectively.

These formulas were first presented by Ludwig (1943) Eqs. (62) to (65) but have not been brought to the forefront of public attention in the geodetic community. Nevertheless, Eqs. (19) and (20) give explicit expressions of the GK projection in another way by the auxiliary variables (α, β) and, connected by Eq. (15), are equivalent to Lee’s formulas.

Finally, the meridian scale k and convergence γ can also be expressed in terms of elliptic functions as (for elaborate derivations see Lee 1963)

$$\begin{cases} k = \frac{\sqrt{1 - e^2 \sin^2 \varphi}}{\cos \varphi} \frac{\sqrt{1 - \operatorname{sn}^2 u \operatorname{dn}'^2 v}}{\sqrt{\operatorname{dn}^2 u + \operatorname{dn}'^2 v - 1}} \\ \tan \gamma = -(1 - e^2) \operatorname{sd} u \operatorname{nc} u \operatorname{sd}' v \operatorname{cn}' v. \end{cases} \tag{21}$$

Obviously, by Lee’s formulas, the inverse solutions of Eqs. (14) and (13) are required for the forward and reverse mapping, respectively. For the forward mapping, the inverse series of Eq. (14) provided by Lee (1962) Eq. (28) has been verified to converge slowly, accompanied by some drawbacks, by Dozier (1980). As to the reverse mapping, there are still no direct formulas to invert Eq. (13). For these reasons, various iterative methods in the complex plane are always used to deal with the two vital inversions (e.g., Dozier 1980;

Karney 2011). However, even though the complex arithmetic iterative procedure shows well-behaved characteristics for computing the mapping, this method is inconvenient for practical applications since complex arithmetic is not often used in surveying and mapping engineering fields.

Although Lee’s method is not typically used in the geodetic community, his work is considered essential for a theoretical deepening of the GK projection, especially for the entire property. In our opinion, developing straightforward procedures for computation of both the forward and inverse mappings is helpful for better understanding of the GK projection.

2.2 Expressions of (u, v) in terms of (Ω, λ)

If the incomplete elliptic integral of the first kind u is redefined in terms of ψ by

$$u = \int_0^\psi p(\psi) d\psi, \tag{22}$$

then the natural extension of the real function u just represents the inverse function of (14), expressed as

$$w = h(\chi) = u + iv = \int_0^{\chi=\psi+i\lambda} p(\chi) d\chi. \tag{23}$$

Here, $p(\psi)$ and $p(\chi)$ remain unknown. However, combining of Eqs. (3) and (10), $p(\psi)$ can be expressed in terms of φ as

$$p(\psi) = p(\psi(\varphi)) = \frac{\cos \varphi \sqrt{1 - e^2 \sin^2 \varphi}}{1 - e^2}. \tag{24}$$

Introducing the conformal latitude (or named spherical latitude)

$$\phi' = \operatorname{gd} \psi = \int_0^\psi \operatorname{sech} \psi \ d\psi = \operatorname{arcsin}(\tanh \psi) \tag{25}$$

as an intermediate auxiliary variable (where $\operatorname{gd} \psi$ is the Gudermannian function, see Olver et al. 2010 §4.23), we have

$$\begin{aligned} \sin \phi' &= \tanh \psi \\ &= \tanh(\operatorname{arctanh}(\sin \varphi) - e \operatorname{arctanh}(e \sin \varphi)). \end{aligned} \tag{26}$$

Subsequently, using the Lagrange inversion theorem (e.g, Olver et al. 2010 §1.10 VII), we derive the relations

$$\begin{cases} \sin \phi' = \left(\frac{1 - n}{1 + n} \right)^2 \sum_{j=1}^\infty a_j \sin^{2j-1} \varphi \\ \sin \varphi = \left(\frac{1 + n}{1 - n} \right)^2 \sum_{j=1}^\infty a'_j \sin^{2j-1} \phi', \end{cases} \tag{27}$$

where the third flattening n , defined by

$$n = \frac{a - b}{a + b} = \frac{1 - \sqrt{1 - e^2}}{1 + \sqrt{1 - e^2}}, \tag{28}$$

is used as an alternative to the first eccentricity e to accelerate the convergence of the series’ coefficients since $n \approx e^2/4$, which is much less than the first eccentricity e .

We should note that, including the derivation of Eq. (27), most complicated mathematical manipulations encountered in this paper are carried out by using the computer algebra system Mathematica (Wolfram 2017). All relevant source codes are available in the electronic supplement and released under the X/MIT open source license (<https://opensource.org/licenses/MIT>).

Substituting the second formula of Eq. (27) into Eq. (24), and after some simplifications, we obtain

$$p(\psi) = F_K \cos \phi' \left(1 + \sum_{j=1}^{\infty} b_j \cos (2j\phi') \right), \tag{29}$$

where F_K denotes the special type of Gaussian hypergeometric functions related to the complete elliptic integral of the first kind (e.g., Cuyt et al. 2008 Eq. (15.1.4)):

$$F_K = {}_2F_1\left(\frac{1}{2}, \frac{1}{2}; 1; e^2\right) = \frac{2}{\pi} K = (1 + n) \left(1 + \frac{n^2}{4} + \frac{9n^4}{64} + \frac{25n^6}{256} + \frac{1225n^8}{16384} + \dots \right). \tag{30}$$

In order to clarify the layout structure of the document, the preceding several terms of coefficients a_j , a'_j and b_j are listed in Eqs. (66) to (68) in “Appendix” and are used as listed hereinafter.

Further, considering that

$$\begin{cases} \cos \phi' = \sqrt{1 - \sin^2 \phi'} = \operatorname{sech} \psi \\ \cos 2\phi' = \cos^2 \phi' - \sin^2 \phi' = 2 \operatorname{sech}^2 \psi - 1 \\ \cos 4\phi' = \cos^4 \phi' - 6 \sin^2 \phi' \cos^2 \phi' + \sin^4 \phi' \\ \quad = 8 \operatorname{sech}^4 \psi - 8 \operatorname{sech}^2 \psi + 1 \\ \dots, \end{cases} \tag{31}$$

series (29) can be reduced to

$$p(\psi) = F_K \sum_{j=1}^{\infty} c_j \operatorname{sech}^{2j-1} \psi. \tag{32}$$

Finally, integrating series (32) term-by-term and extending the real isometric latitude ψ to the complex form $\chi = \psi + i\lambda$, we obtain

$$\begin{aligned} w &= u + iv \\ &= F_K \left(\arcsin (\tanh \chi) + \tanh \chi \sum_{j=1}^{\infty} d_j \operatorname{sech}^{2j-1} \chi \right) \\ &= F_K \left(\phi'_c + \sum_{j=1}^{\infty} f_j \sin (2j\phi'_c) \right), \end{aligned} \tag{33}$$

where ϕ'_c represents the complex conformal latitude, defined by

$$\begin{aligned} \phi'_c &= \xi' + i\eta' = \arcsin (\tanh \chi) \\ &= \arctan \left(\frac{\sinh \psi}{\cos \lambda} \right) + i \operatorname{arctanh} \left(\frac{\sin \lambda}{\cosh \psi} \right). \end{aligned} \tag{34}$$

Separating the real and imaginary parts of Eq. (33), we have

$$\begin{cases} u = F_K \left(\xi' + \sum_{j=1}^{\infty} f_j \sin (2j\xi') \cosh (2j\eta') \right) \\ v = F_K \left(\eta' + \sum_{j=1}^{\infty} f_j \cos (2j\xi') \sinh (2j\eta') \right). \end{cases} \tag{35}$$

By series (33) or (35), the forward mappings of both the GK and Thompson projections can be implemented without iteration.

Additionally, with similar procedures, the perturbation series described by Bermejo-Solera and Otero (2009) for the GK projection can be expanded and rearranged to higher orders as

$$\begin{aligned} z &= x + iy \\ &= aF_E \left(\arcsin (\tanh \chi) + \tanh \chi \sum_{j=1}^{\infty} g_j \operatorname{sech}^{2j-1} \chi \right) \\ &= aF_E \left(\phi'_c + \sum_{j=1}^{\infty} h_j \sin (2j\phi'_c) \right), \end{aligned} \tag{36}$$

where F_E denotes the special type of Gaussian hypergeometric functions related to the complete elliptic integral of the second kind, defined by

$$\begin{aligned} F_E &= {}_2F_1\left(\frac{1}{2}, -\frac{1}{2}; 1; e^2\right) = \frac{2}{\pi} E \\ &= \frac{1}{1 + n} \left(1 + \frac{n^2}{4} + \frac{n^4}{64} + \frac{n^6}{256} + \frac{25n^8}{16384} + \dots \right), \end{aligned} \tag{37}$$

and h_j is equal to α_j in (Karney 2011 Eq. (35)); therefore, we do not list these coefficients in this article. The coefficients c_j to g_j are also listed in “Appendix,” from Eqs. (69) to (72).

Separating the real and imaginary parts of Eq. (36), we obtain the “Krüger- n ” series

$$\begin{cases} x = a F_E \left(\xi' + \sum_{j=1}^{\infty} h_j \sin(2j\xi') \cosh(2j\eta') \right) \\ y = a F_E \left(\eta' + \sum_{j=1}^{\infty} h_j \cos(2j\xi') \sinh(2j\eta') \right). \end{cases} \quad (38)$$

Notably, the constant F_E is usually signified by R , A or another capital letter in the previous literature, e.g., in Bermejo-Solera and Otero (2009) and Karney (2011). We consider that using F_E to denote the constant F_E better embodies its mathematic essence: F_E represents the abbreviation of the Gaussian hypergeometric function ${}_2F_1\left(\frac{1}{2}, \frac{1}{2}; 1; e^2\right)$, which is related to the complete elliptic integral of the second kind $E = E(\pi/2, e)$, as defined in Eq. (37). This is also the case for F_K .

2.3 Series approximations for (x, y) in terms of (u, v)

In practical applications, it is often necessary to develop fast-converging series approximations to calculate the rectangular coordinates (x, y) in terms of (u, v) , since the elliptic functions and integrals encountered in Eq. (16) usually must be coded by series or other algorithms in a computer program. A type of Taylor series in terms of w was first derived by Lee (1962) Eq. (29) and then transformed in terms of complex isometric latitude χ by his Eq. (30). It was verified by Dozier (1980) that the series are difficult to use due to some drawbacks, especially the slow convergence of the series. In this subsection, the q -series approximations provided by Dozier (1980) are simplified to a more concise form, and new formulas for the reverse mapping based on this form are derived in the next subsection.

In the theory of elliptic functions, the nome q is defined by (e.g, Olver et al. 2010 §22.2)

$$q = \exp\left(-\frac{\pi K'}{K}\right) \quad (39)$$

and the Jacobian zeta function $Z(w)$ is expressed as

$$Z(w) = Z(w, e) = \frac{2\pi}{K} \sum_{j=1}^{\infty} \frac{q^j}{1 - q^{2j}} \sin\left(\frac{j\pi w}{K}\right). \quad (40)$$

In these two formulas, $K = F(\pi/2, e)$ and $K' = F\left(\pi/2, \sqrt{1 - e^2}\right)$ are the complete elliptic integral of the first kind, with the complementary moduli e and $\sqrt{1 - e^2}$, respectively.

According to the relation between the elliptic integral of the second kind and the Jacobian zeta function

$$E(w) = Z(w) + \frac{wE}{K}, \quad (41)$$

the GK projection can be expressed as

$$\begin{aligned} z = x + iy &= aE(K + w) - aE \\ &= aZ(K + w) + \frac{a(K + w)E}{K} - aE \\ &= \frac{awE}{K} + \frac{2a\pi}{K} \sum_{j=1}^{\infty} \frac{(-q)^j}{1 - q^{2j}} \sin\left(\frac{j\pi w}{K}\right). \end{aligned} \quad (42)$$

If

$$\begin{cases} \phi_c = \frac{z}{aF_E} = \frac{x + iy}{aF_E} = \xi + i\eta \\ \zeta_c = \frac{w}{F_K} = \frac{u + iv}{F_K} = \theta + i\vartheta, \end{cases} \quad (43)$$

then Eq. (42) is equivalent to

$$\phi_c = \zeta_c + \frac{\pi^2}{KE} \sum_{j=1}^{\infty} \frac{(-q)^j}{1 - q^{2j}} \sin(2j\zeta_c). \quad (44)$$

Multiplying aF_E on both sides of Eq. (44) and splitting the equation into real and imaginary parts give

$$\begin{cases} x = aF_E \left(\theta + \frac{\pi^2}{KE} \sum_{j=1}^{\infty} \frac{(-q)^j}{1 - q^{2j}} \sin(2j\theta) \cosh(2j\vartheta) \right) \\ y = aF_E \left(\vartheta + \frac{\pi^2}{KE} \sum_{j=1}^{\infty} \frac{(-q)^j}{1 - q^{2j}} \cos(2j\theta) \sinh(2j\vartheta) \right). \end{cases} \quad (45)$$

Equations (42) and (45) give infinite series expressions for the GK projection that are suitable for computer processing.

3 New formulas for reverse mapping based on Lee’s exact method

According to Lagrange’s inversion theorem, the inverse series of Eq. (44) is given by

$$\zeta_c = \phi_c + \sum_{j=1}^{\infty} \frac{1}{j!} \frac{d^{j-1}}{d\phi_c^{j-1}} \left\{ [G(\phi_c)]^j \right\}, \quad (46)$$

where

$$\begin{aligned} G(\phi_c) &= -\frac{\pi}{2E} Z(K + w_z) \\ &= -\frac{\pi^2}{KE} \sum_{j=1}^{\infty} \frac{(-q)^j}{1 - q^{2j}} \sin(2j\phi_c) \end{aligned} \quad (47)$$

and

$$w_z = F_K \phi_c = \frac{Kz}{aE}. \quad (48)$$

In order to derive the previous several terms of Eq. (46), we first expand the nome q in terms of the third flattening n as

$$q = \exp\left(-\frac{\pi K'}{K}\right) = \frac{n}{4} + \frac{n^3}{16} + \frac{17n^5}{512} + \frac{45n^7}{2048} + \dots, \quad (49)$$

and substitute Eq. (49) into Eq. (47); then, the function $G(\phi)$ can be rearranged as

$$G(\phi_c) = \sum_{j=1}^{\infty} k_j \sin(2j\phi_c). \quad (50)$$

After substituting Eq. (50) into Eq. (46) and conducting a tedious derivation procedure, we finally obtain the inverse function of Eq. (44):

$$\zeta_c = \phi_c + \sum_{j=1}^{\infty} l_j \sin(2j\phi_c), \quad (51)$$

where the terms of the coefficients k_j and l_j are listed in Eq. (73) in “Appendix”.

Multiplying F_K on both sides of Eq. (51), we have

$$w = u + iv = F_K\left(\phi_c + \sum_{j=1}^{\infty} l_j \sin(2j\phi_c)\right). \quad (52)$$

Splitting Eq. (52) into real and imaginary parts gives

$$\begin{cases} u = F_K\left(\xi + \sum_{j=1}^{\infty} l_j \sin(2j\xi) \cosh(2j\eta)\right) \\ v = F_K\left(\eta + \sum_{j=1}^{\infty} l_j \cos(2j\xi) \sinh(2j\eta)\right). \end{cases} \quad (53)$$

In conjunction with Eqs. (43), (52) and (53), one can obtain the values of the intermediate coordinates (u, v) from the given GK coordinates (x, y) and then easily calculate (ψ, λ) by using Eqs. (14) or (17). Finally, in the last step of the inverse mapping, the geodetic latitude φ is calculated from the isometric latitude ψ , usually by iterative procedures. As an alternative method to various iterative algorithms, here we provide a series approximation for the task by

$$\begin{aligned} \varphi &= \psi^{-1}(\psi) \\ &= \arcsin(\tanh \psi) + \tanh \psi \sum_{j=1}^{\infty} m_j \operatorname{sech}^{2j-1} \psi, \end{aligned} \quad (54)$$

where $\psi^{-1}(\psi)$ denotes the inverse function of Eq. (3), and $m_1 \sim m_8$ are itemized in Eq. (74) in “Appendix.”

4 Precision and efficiency evaluation

To clearly articulate the GK forward and reverse mapping procedures via Lee’s formulas, we extract the main steps from the tedious derivations as follows:

- (1) for the forward mapping, the procedure is

$$(\varphi, \lambda) \xrightarrow{\text{Eq.(3)}} (\psi, \lambda) \xrightarrow[\text{or (35)}]{\text{Eq.(33)}} (u, v) \xrightarrow[\text{or (16), or (45)}]{\text{Eq.(13) or (42)}} (x, y), \quad (55)$$

- (2) and likewise, the reverse process is

$$(x, y) \xrightarrow[\text{or (53)}]{\text{Eq.(52)}} (u, v) \xrightarrow[\text{or (17)}]{\text{Eq.(14)}} (\psi, \lambda) \xrightarrow{\text{Eq.(54)}} (\varphi, \lambda). \quad (56)$$

To demonstrate the procedures better, two examples of the coordinate calculations, forward mapping following the procedure (55) by given $(\varphi = 60^\circ, \lambda = 3^\circ)$ and reverse mapping following (56) by given $(x = 6.657E6m, y = 1.670E5m)$, were implemented and the results are shown in Table 1. All examples and tests in this article were implemented with the GRS80 ellipsoid data ($a = 6378137m$ and $f = 1/298.257222101$).

Following these procedures, the precisions of the forward and reverse mappings obviously mainly depend on the truncation of series (33), (42), (52) (or their real and imaginary parts separated forms (35), (45), (53), respectively) and (54). However, as described by Karney (2011), the overall errors of numerical computations are the combined effect of the truncation error (caused by truncating and approximating an infinite sum by a finite sum) and the round-off error (caused by using finite precision floating-point numbers in computers). Thus, it is necessary to quantify and distinguish these two types of errors in applications.

Since elliptic functions and integrals can be calculated to an arbitrary accuracy by using the computer algebra system Mathematica (Wolfram 2017), we first determine the truncation error in Mathematica by using the option

Table 1 Examples of the coordinate calculations following the procedures (55) and (56)

Coordinates	Values	
	Forward mapping	Reverse mapping
φ	60°	$59^\circ 59' 32.499976''$
λ	3°	$2^\circ 59' 34.158300''$
ψ	1.311151	1.310884
u	1.048826	1.048690
v	0.026284	0.026227
x	6657868.630965 m	6657000.000000 m
y	167361.765833 m	167000.000000 m

“WorkingPrecision” to eliminate the effect of round-off errors. The concrete strategy for determining the truncation error is as follows:

Given the arbitrary (α, β) (which corresponds one-to-one to (φ, λ) by Eq. (20)), first, the exact values of (x, y) and (ψ, λ) can be obtained by Eqs. (19) and (20). Meanwhile, the approximations of these values, denoted by (x', y') and (ψ', λ') , can be calculated following the forward and reverse processes (55) and (56), respectively. Then, their absolute errors can be determined by the discrepancies between the approximate and actual values, denoted as $\delta_x = |x' - x|$, $\delta_y = |y' - y|$, $\delta_\psi = |\psi' - \psi|$ and $\delta_\lambda = |\lambda' - \lambda|$, respectively.

With respect to the precision of φ in the reverse mapping, we extend series Eq. (54) to a higher order to calculate φ by using exact values of ψ (the 16th order was implemented in our test). Thus, the loss of precision is of little consequence to lower orders and can be ignored. Assuming the results obtained by this route are the actual values of φ , then the absolute errors of approximations of φ' obtained from the reverse mapping process are determined by $\delta_\varphi = |\varphi - \varphi'|$.

Finally, we use the positional errors of point

$$\begin{cases} \delta_p = \sqrt{\delta_x^2 + \delta_y^2} \\ \delta'_p = \sqrt{[M(\varphi)]^2 \delta_\varphi^2 + [N(\varphi) \cos \varphi]^2 \delta_\lambda^2} \end{cases} \quad (57)$$

to evaluate the precisions of the forward and reverse mappings, respectively, where $M(\varphi)$ and $N(\varphi)$ represent the meridian and prime vertical radius of curvature of the ellipsoid:

$$\begin{cases} M(\varphi) = \frac{a(1 - e^2)}{(1 - e^2 \sin^2 \varphi)^{3/2}} \\ N(\varphi) = \frac{a}{\sqrt{1 - e^2 \sin^2 \varphi}} \end{cases} \quad (58)$$

Following this strategy, the precisions of the forward and reverse mappings are tested with the GRS80 ellipsoid in the range of $-89^\circ \leq \alpha \leq +89^\circ$ and $-80^\circ \leq \beta \leq +80^\circ$, i.e., the region highlighted with a blue boundary in Fig. 1.

In Fig. 2a, b, the maximum truncation errors of the forward and reverse mappings are plotted as functions of $|\beta|$ at various orders ranging from 2 to 12.

Furthermore, the round-off error caused by floating-point arithmetic is evaluated by machine epsilon $\epsilon_m = 2^{-(p-1)}$ as $\delta_r \approx 2Q\epsilon_m = Q/2^{p-2}$ (Karney 2011), where $Q = 10000\text{km}$ represents the length of the meridian quadrant of the earth, and p is the number of bits in the fraction of the floating-point number system. Similar to Karney’s prescription, we implement the algorithms with double ($p = 53$) and extended ($p = 64$) precisions at n^6 and n^7 orders, respectively, and the overall numerical errors (truncation and

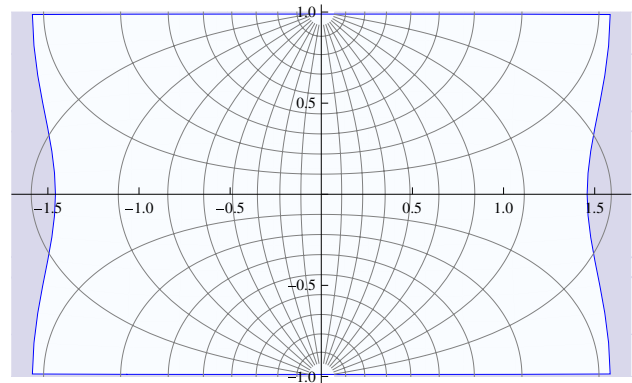


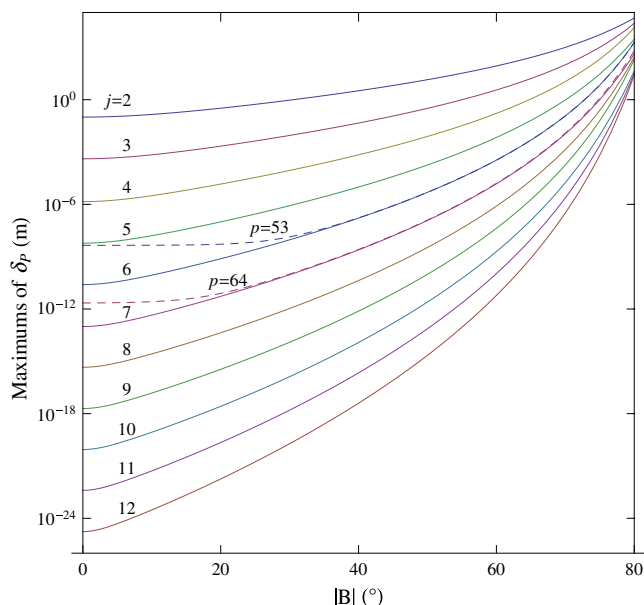
Fig. 1 Precision test region for the forward and reverse mappings following the procedures of (55) and (56). The region is highlighted with a blue boundary. GRS80 ellipsoid data are used in the test, and the mapping of the central meridian quadrant is scaled to unity. The graticule is portrayed at 10° intervals

round-off) are plotted as dashed lines in Fig. 2. The results illustrate that the round-off errors with double (resp. extended) precision can be neglected, while the algorithms are implemented at no more than order n^5 (resp. n^6).

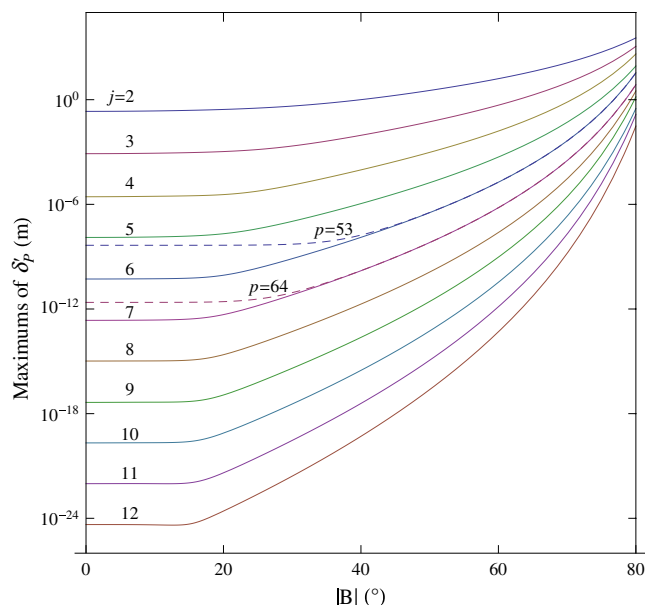
In comparison with the extended Krüger- n series provided and tested by Karney (2011), Fig. 2 shows that the new algorithms reach an equivalent precision level as the Krüger- n series for the same orders and have distinct advantages over the Krüger- λ series. Normally, within the standard UTM 6° zone width, the maximum errors of the new algorithms with an order of n^3 or n^4 are less than 0.42mm or 1.47 μm for the forward mapping and 0.81mm or 2.73 μm for the reverse mapping, respectively. These levels of precision are adequate for most applications, and, if higher precisions or wider zones are required, the algorithms can be implemented at higher orders; the corresponding precisions of orders up to n^{12} are shown in Fig. 2.

In a similar manner, it was shown by our test that the complex latitude methods are also at the same precision level with the Krüger- n series and the new method for the same orders. For brevity, we shall not repeat the test here.

As to the efficiency and algorithmic complexity, it can be foreseen that the new algorithms’ performances will be inferior to the Krüger- n series since more parameters and variables, including $F_K, \theta, \vartheta, q$ and several coefficients in terms of q , are additionally needed in the new algorithms. Nevertheless, for reference, we still compared the efficiency of new algorithms with the Krüger- n series and the complex latitude method (for more details of the complex latitude method, see Poder and Engsager 1998). Only forward mappings implemented by the three methods are compared since the reverse mappings have the same procedures with the forward mappings.



(a) Truncation and round-off errors for the forward mapping



(b) Truncation and round-off errors for the reverse mapping

Fig. 2 Maximum truncation and round-off errors as functions of $|\beta|$ **a** for the forward GK mapping following the procedure of (55) and **b** for the reverse GK mapping following the procedure of (56) at various orders j from 2 to 12. The solid lines show the truncation

errors, and the dashed lines show the combined truncation and round-off errors for double precision ($p = 53$ bits) and extended precision ($p = 64$ bits) at the orders $j = 6$ and $j = 7$, respectively

Table 2 CPU times of the three algorithms for the forward mapping of the GK projection (Unit: microsecond (μs))

Method	Test set		
	A	B	C
Krüger- n series	0.35	0.34	0.33
Complex latitude method	0.54	0.54	0.53
New method following (55)	0.55	0.55	0.54

Shown are the averaged CPU times for calculating a GK coordinates (x, y) from a given geodetic coordinates (φ, λ) by the Krüger- n series method, the complex latitude method and the new method following the procedure (55) at n^4 order, respectively. They were evaluated by averaging the CPU time measurements for three sets of equally spaced grid points of (φ, λ) , which are obtained by varying the latitude and longitude in the range $\{-88^\circ \leq \varphi \leq +88^\circ, -15^\circ \leq \lambda \leq +15^\circ\}$ with steps of $0.1^\circ, 0.05^\circ$ and 0.01° , i.e., 530601, 2116121 and 52822601 points in total for sets A, B and C, respectively. The programming language used in the measurements was Microsoft Visual C++, run on PC with Inter(R) Core(TM)i7-4810MQ CPU@2.80GHz, 32 GB RAM, Windows 10 operation system

The results from time efficiency testing presented in Table 2 show that the new method runs with the same level of the complex latitude method and slower about 0.19 to 0.21 μs per point than the Krüger- n series method. However, our purpose of developing straightforward procedures for both forward and reverse mapping of the GK projection

based on Lee’s exact method is mainly focused on to reveal the essence of the GK projection, as elaborately discussed in Sect. 5.

5 Complements of the GK projection’s properties

As summarized by Grafarend and Syffus (1998), the GK projection is essentially generated by a two-step procedure: (1) deriving conformal coordinates (ψ, λ) from geodetic coordinates (φ, λ) and (2) transforming the conformal coordinates (ψ, λ) into the GK coordinates (x, y) by means of the holomorphic function $w = u + iv$. Equivalently, if the calculation of intermediate projection $w = u + iv$ is considered an independent step, the two-step procedure can be regarded as a three-step procedure, as shown in Eq. (55) and Fig. 3. However, the procedure cannot have a one-to-one correspondence and be conformal over the entire ellipsoid, since, for the global coverage of the ellipsoid, there must be at least two maps to avoid singularities (Grafarend et al. 2014), or in another word, any map over the entire ellipsoid has at least one singularity since, from the topological principles, the punctured sphere (denoted by $(S^2 - p)$, a two-dimensional Riemann manifold) is homeomorphic to the two-dimensional Euclidean plane \mathbb{R}^2 (e.g., Munkres 2000 Theorem 59.3).

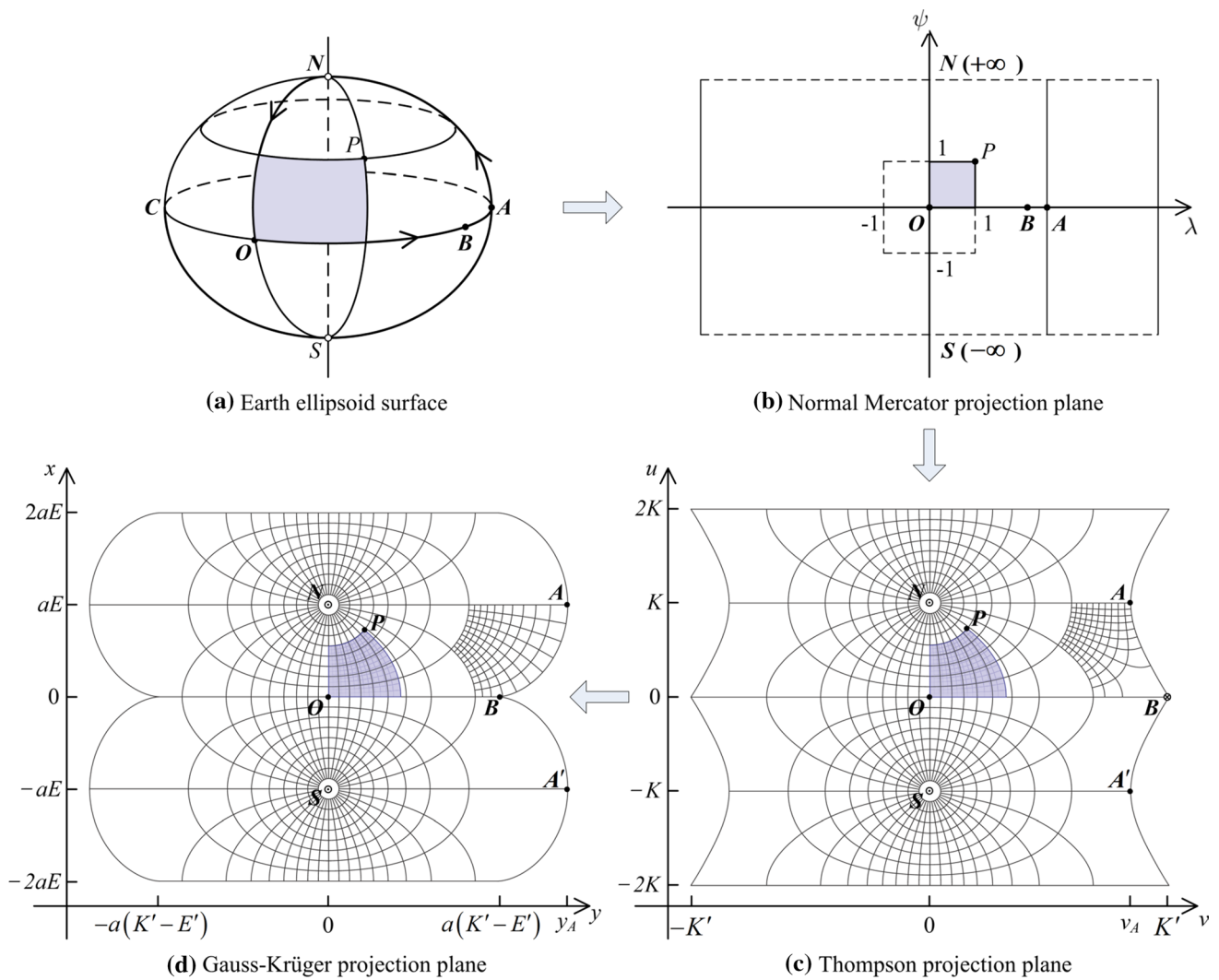


Fig. 3 Illustration of the three-step procedure of the GK projection. Here, the graticule in the Normal Mercator projection is omitted, and in the Thompson and GK projections, the graticule is shown at multiples of 10° with 1° lines added in $80^\circ < \lambda < 90^\circ$ and $0^\circ < \varphi < 10^\circ$. In

particular, the shallowed regions are used to illustrate the projected shapes of the unit isothermal coordinates ($\psi_p = 1, \lambda_p = 1$) in the Normal Mercator, Thompson and GK projections

In fact, following convention, the standard GK projection over the entire ellipsoid is mapped by gluing three charts together: One chart covers the hemisphere in which the meridians at 90° east and west of the chosen central meridian are projected to horizontal lines through the poles, and the other two charts cover the more distant hemisphere by dividing and projecting it into two equal parts above the north pole and below the south pole, as shown in Fig. 3d.

A simple method to obtain the exhaustive properties of projections over the entire ellipsoid is to analyze the procedure from the perspective of complex analysis. Due to symmetry, it is sufficient to consider one quadrant of a hemispheroid. Here, we suppose a point starts at O and moves on the boundary of a quadrant of the northern hemispheroid anticlockwise, as shown in Fig. 3a, along the direction of

the arrow; the geodetic and projected coordinates of the point consequently vary along the boundary. The variations are shown in Table 3, where $\lambda_b = (1 - e)\pi/2$ is analyzed in detail by Lee (1962) and Karney (2011), and v_A and y_A are determined by

$$\psi_A = \operatorname{arctanh}(\operatorname{dn}' v_A) - e \operatorname{arctanh}(e \operatorname{nd}' v_A) = 0 \quad (59)$$

and

$$y_A = av_A - aE'(v_A) + \frac{a(1 - e^2) \operatorname{sn}' v_A \operatorname{cn}' v_A \operatorname{dn}' v_A}{-e^2 + \operatorname{dn}'^2 v_A}, \quad (60)$$

respectively.

Table 3 Coordinate variations on the boundary of the Northern Hemi-spheroid quadrant

Coordinates	Loop			
	<i>O</i> to <i>B</i>	<i>B</i> to <i>A</i>	<i>A</i> to <i>N</i>	<i>N</i> to <i>O</i>
φ	0	0	0 to $\pi/2$	$\pi/2$ to 0
λ	0 to λ_B^*	λ_B to $\pi/2$	$\pi/2$	0
ψ	0	0	0 to $+\infty$	$+\infty$ to 0
<i>u</i>	0	0 to <i>K</i>	<i>K</i>	<i>K</i> to 0
<i>v</i>	0 to <i>K'</i>	<i>K'</i> to v_A^*	v_A to 0	0
<i>x</i>	0	0 to <i>aE</i>	<i>aE</i>	<i>aE</i> to 0
<i>y</i>	0 to $a(K' - E')$	$a(K' - E')$ to y_A^*	y_A to 0	0

* $\lambda_B = (1 - e)\pi/2$; v_A and y_A are determined by Eqs. (59) and (60), respectively

Setting $k_v = v_A/K'$ and $k_y = a(K' - E')/y_A$, then $k_v \approx 0.84016080618551$ and $k_y \approx 0.70822383771793$, as obtained from the GRS80 parameters. The two proportions referring to GRS80 show general features of the boundaries of the Thompson and GK projections for the Earth ellipsoid.

In mathematics, coordinates of a two-dimensional Riemann manifold (temporarily denoted as (μ, ν)) in which the square of the line element has the form

$$ds^2 = \rho^2(\mu, \nu)(d\mu^2 + d\nu^2) \tag{61}$$

with $\rho^2(\mu, \nu) > 0$ smooth are named isothermal coordinates (e.g., Hazewinkel 2012).

This means that isothermal coordinates of a two-dimensional Riemann manifold specify a conformal mapping of the two-dimensional Riemann manifold into the two-dimensional Euclidean plane. Specializing to the map projection case, the isometric latitude ψ and the longitude λ are essentially the isothermal coordinates (ψ, λ) on the ellipsoid surface and the square of the line element is given by

$$ds^2 = [M(\varphi)d\varphi]^2 + [N(\varphi) \cos \varphi d\lambda]^2 = r^2(\psi)(d\psi^2 + d\lambda^2) \tag{62}$$

with $r^2(\psi) > 0$ smooth, where the south and north poles are excluded since $r(\psi) = 0$ at the poles.

In particular, Eq. (62) is converted to $ds = r(\psi)d\psi$, i.e., the differential of the meridian arc, in the case $\lambda = \text{constant}$. Integrating $ds = r(\psi)d\psi$ and extending it to the complex plane, it is the definition of the GK projection, expressed by Eqs. (1) to (3).

Significantly, the step deriving isothermal coordinates (ψ, λ) from geodetic coordinates (φ, λ) essentially determines a conformal mapping (i.e., the Normal Mercator projection) of the ellipsoid surface (excluding the south and north poles, considering as a two-dimensional Riemann manifold) into the Euclidean plane, as shown from Fig. 3a,

b. The step is the foundation of the following two steps and also plays a particularly important role in other conformal projections.

Suppose point $P(\varphi_p, \lambda_p)$ is located by

$$\begin{cases} \psi_p = \operatorname{arctanh}(\sin \varphi_p) - e \operatorname{arctanh}(e \sin \varphi_p) = 1 \\ \lambda_p = 1, \end{cases} \tag{63}$$

then the region on the ellipsoid surface bounded by meridian λ_p and the initial meridian, the parallel φ_p and the equator is projected to a unit square grid in the Normal Mercator projection, as shown from Fig. 3a, b. Also taking the GRS80 ellipsoid as an example, it can be calculated that $\varphi_p \approx 49^\circ 47' 40.76''$ and $\lambda_p = 180^\circ/\pi$. The unit square grid typically illustrates the role of the isothermal coordinates, and the shapes of the same region projected in Fig. 3b, c, d show that all three projections preserve angles but distort sizes and areas.

However, on the maps of the entire ellipsoid there are singularities at which local angles are distorted. Firstly, the south and north poles are singularities of the Normal Mercator projection, since $\psi \rightarrow \pm\infty$ when points approach the poles, as shown in Fig. 3b. Furthermore, considering the derivatives of the projection functions (1) and (23),

$$\begin{cases} S'(\chi) = \frac{dz}{d\chi} = a \operatorname{sn}(K + w) \\ h'(\chi) = \frac{dw}{d\chi} = \frac{\operatorname{cn} w \operatorname{dn} w}{(1 - e^2)}, \end{cases} \tag{64}$$

it can be concluded that $S'(\pm K) = 0$ and $h'(\pm K) = 0$. Therefore, the GK and Thompson projections are both un-conformal at the south and north poles.

In the same manner, it can be obtained that $S'(iK') = a/e$ and $h'(iK')$ does not exist. This indicates that the GK projection is conformal at point *B*, while the Thompson projection is not.

In addition, because of $\psi = 0$ and $(1 - e)\pi/2 \leq \lambda \leq \pi/2$ in the segment *BA* on the equator, so that, from Eq. (17) we have

$$\begin{cases} \operatorname{arctanh}(\operatorname{sn} u \operatorname{dn}' v) = e \operatorname{arctanh}(e \operatorname{sn} u \operatorname{nd}' v) \\ \lambda = \operatorname{arctan}(\operatorname{dc} u \operatorname{sc}' v) - e \operatorname{arctan}(e \operatorname{cd} u \operatorname{sc}' v), \end{cases} \tag{65}$$

which is not a one-to-one correspondence in the domain $\{\psi = 0, (1 - e)\pi/2 < \lambda \leq \pi/2\}$ since, if a pair of coordinates (u, v) satisfy Eq. (65), then $(-u, v)$ also satisfy. It is the reason that the two projections, Thompson and GK, are multi-valued from the branch points *B* to *A* on the equator, and thus, the condition of holomorphic bijection for the two projections fails in the segment (for more elaborate discussions see Lee 1962; Karney 2011).

If a function $z = f(w)$ maps a region *D* bounded by a simple closed curve *C* in the *w*-plane conformally upon a

corresponding region Δ bounded by a closed curve Γ in the z -plane, and the region D is small enough for the corresponding region Δ to consist of the entire z -plane without overlapping, the region D is called a fundamental region of the w -plane for the function $f(w)$ (Bowman (1961) Chap. V, §1). Equivalently, the definition means that the region D is the maximum open, connected and non-empty set in the w -plane on which the function $f(w)$ defines a conformal mapping without singularities.

Synthetically considering the features discussed above and using the “fundamental region of conformal map” concepts defined by Bowman (1961), we finally determine the fundamental regions of the three projections, as shown in Table 4.

Mathematically, the fundamental region of a conformal map is also usually named a fundamental domain, in which the mapping is biholomorphic, namely conformal without singularities. At this point, the domain of the GK projection raised in Sect. 1 is determined.

6 Conclusion

It was shown that the three definitions of the GK projection, defined by the complex isometric latitude, the complex latitude and Lee’s analytical functions respectively, are equivalent. However, as analyzed above, truncated series that are generated by the first definition, e.g., Krüger- λ and Krüger- n series, are generally used in practical applications, while exact mappings expressed by Lee’s analytical functions are rare. Due to its infrequent use, the importance of Lee’s exact method was somewhat neglected.

Typically, the characterization of both the local and global features of the GK projection cannot be accomplished competently by only the first two definitions or any series expansion methods. Instead, Lee’s formulation is necessary since it explicitly defines the projection by analytical functions. In addition, the derivative of the first definition, which must be nonzero for conformality, can be expressed exactly only by Lee’s formulas.

The algorithms presented here allow both forward and inverse mappings of the GK projection to be implemented without complex iterative procedures based on Lee’s exact method, which essentially reveal the mapping procedures

and intrinsic properties of the GK projection. As a summary, we highlight the major conclusions here:

- (1) One of the most concise manners of defining the conformal map in geodesy and cartography is using analytical complex-valued functions by which it can be found that the Cauchy–Riemann equations, together with certain continuity and differentiability criteria, form a necessary and sufficient condition for a complex function to be complex differentiable, i.e., holomorphic, necessary but not sufficient for conformality.
- (2) Indispensable but almost ignored in the geodetic community that the derivative of a conformal projection’s function should be nonzero everywhere on the domain is also a necessary condition for conformality.
- (3) The first definition of the GK projection described in Sect. 1 is a generic definition for conformal maps, i.e., a mapping is conformal if and only if its function is biholomorphic on an open, connected and non-empty set.
- (4) Because the non-punctured sphere or ellipsoid is not homeomorphic to the Euclidean plane, any map projection has at least one singularity in mapping the entire Earth surface, and thus, it is necessary to determine the domain of a map projection.

Based on these recognitions and the “three-step procedure” of the GK projection, the conformality and singularities over the entire ellipsoid of the Normal Mercator, Thompson and GK projections were analyzed and the fundamental domains of them were determined.

Finally, with respect to the precision and efficiency of new algorithms, it was verified that the new algorithms had equivalent precision levels for the same orders with the Krüger- n series but rather slower than the Krüger- n series. So, considering the lower-level efficiency, we are not intended to recommend the new algorithms in practical applications for the GK projection. However, we think the usefulness of the new formulas lies in the procedure, including Eqs. (33), (35), (42), (45), (52) and (53), provided series approximations for the forward mapping of the Thompson projection and projective transformations for the Normal Mercator, Thompson and GK projections.

Acknowledgements We would like to express our gratitude to the anonymous reviewers, the responsible editor and the Editor-in-Chief, Jürgen Kusche, for their insightful comments and suggestions, which greatly helped to improve our manuscript. We thank Dr. Yi Liu (Institute of Geographic Sciences and Natural Resources, CAS) for the helpful discussions. This study was supported by the National Natural Science Foundation of China (Grant Nos. 41631072, 41504031, 41721003, 41574007 and 41429401), the Discipline Innovative Engineering Plan of Modern Geodesy and Geodynamics (Grant No. B17033) and the DAAD Thematic Network Project (Grant No. 57173947).

Table 4 fundamental regions of the Normal Mercator, Thompson and GK projections

Projection	Fundamental region
Normal Mercator	$\{ \varphi < \pi/2, \lambda < \pi\}$
Thompson	$\{ \varphi < \pi/2, \lambda < \pi/2\} - \{\varphi = 0, (1 - e)\pi/2 \leq \lambda < \pi/2\}$
GK	$\{ \varphi < \pi/2, \lambda < \pi/2\} - \{\varphi = 0, (1 - e)\pi/2 \leq \lambda < \pi/2\}$

Author contributions W.B. Shen, J.C. Guo and J.S. Ning designed research; J.C. Guo performed research and wrote the paper; W.B. Shen and J.S. Ning supervised the research and also contributed to the algorithm implementation and result interpretation.

and released under the X/MIT open source license (details see <https://opensource.org/licenses/MIT>). We sadly announce that Prof. J.S. Ning passed away on 15 March 2020 of a chronic disease at the age of 88. He was a distinguished scientist of China and we deeply mourn him.

Data Availability Statement The programs and source codes generated during the current study are available in the electronic supplement

Appendix: Lists of series’ coefficients

$$\left\{ \begin{aligned} a_1 &= 1 \\ a_2 &= \frac{4n(3+2n+3n^2)}{3(1+n)^4} \\ a_3 &= \frac{64n^2(1+n+n^2)(5+2n+5n^2)}{15(1+n)^8} \\ a_4 &= \frac{256n^3(1+n+n^2)}{315(1+n)^{12}} (147 + 172n + 322n^2 + 172n^3 + 147n^4) \\ a_5 &= \frac{1024n^4(1+n+n^2)}{2835(1+n)^{16}} (1881 + 3690n + 7511n^2 + 7436n^3 + 7511n^4 + 3690n^5 + 1881n^6) \\ a_6 &= \frac{4096n^5(1+n+n^2)}{155925(1+n)^{20}} (148005 + 409468n + 954756n^2 + 1316484n^3 + 1600174n^4 \\ &\quad + 1316484n^5 + 954756n^6 + 409468n^7 + 148005n^8) \end{aligned} \right. \tag{66}$$

$$\left\{ \begin{aligned} a'_1 &= 1 \\ a'_2 &= -\frac{4n(3+2n+3n^2)}{3(1-n)^4} \\ a'_3 &= \frac{16n^2(25+32n+62n^2+32n^3+25n^4)}{15(1-n)^8} \\ a'_4 &= -\frac{256n^3}{315(1-n)^{12}} (252 + 473n + 1096n^2 + 1030n^3 + 1096n^4 + 473n^5 + 252n^6) \\ a'_5 &= \frac{256n^4}{2835(1-n)^{16}} (18621 + 45936n + 122524n^2 + 160976n^3 + 212174n^4 + 160976n^5 \\ &\quad + 122524n^6 + 45936n^7 + 18621n^8) \\ a'_6 &= -\frac{1024n^5}{155925(1-n)^{20}} (2185425 + 6672418n + 20019565n^2 + 33138104n^3 + 51507906n^4 \\ &\quad + 53289548n^5 + 51507906n^6 + 33138104n^7 + 20019565n^8 + 6672418n^9 + 2185425n^{10}) \end{aligned} \right. \tag{67}$$

$$\left\{ \begin{aligned} b_1 &= 3n - \frac{4n^2}{3} - \frac{47n^3}{24} + \frac{293n^4}{90} - \frac{241n^5}{720} - \frac{72029n^6}{18900} + \frac{7021093n^7}{1612800} + \frac{5196481n^8}{25401600} - \dots \\ b_2 &= \frac{73n^2}{12} - \frac{76n^3}{15} - \frac{3427n^4}{531n^3} + \frac{6278n^5}{1121n^4} + \frac{6278n^5}{315} - \frac{81547n^6}{69120} - \frac{5357593n^7}{151200} + \frac{348016423n^8}{8709120} + \dots \\ b_3 &= \frac{531n^3}{40} - \frac{15}{70} - \frac{360}{14843n^5} - \frac{144841n^5}{12470017n^6} + \frac{365357n^6}{16018067n^7} - \frac{3427253n^7}{38515416901n^8} - \frac{524932337n^8}{2661120} + \dots \\ b_4 &= \frac{603793n^4}{20160} - \frac{70}{555379n^5} - \frac{4480}{3803159n^6} - \frac{129600}{568876163n^7} + \frac{4320}{51975} - \frac{537600}{64225156139n^8} - \frac{2661120}{958003200} - \dots \\ b_5 &= \frac{8064}{4266870481n^6} - \frac{28512}{885241627n^7} - \frac{2128896}{3440458049657n^8} + \frac{62270208}{4843238400} + \dots \\ b_6 &= \frac{26611200}{37217872147n^7} - \frac{2402400}{44517464099n^8} - \frac{4843238400}{44478720} - \dots \\ b_7 &= \frac{98841600}{41377942693441n^8} - \dots \\ b_8 &= \frac{46495088640}{46495088640} - \dots \end{aligned} \right. \tag{68}$$

$$\begin{cases}
 c_1 = 1 - 3n + \frac{89n^2}{12} - \frac{983n^3}{60} + \frac{669097n^4}{20160} - \frac{85205n^5}{1344} + \frac{4613096261n^6}{39916800} - \frac{7023747629n^7}{34594560} + \frac{241216793515063n^8}{697426329600} - \dots \\
 c_2 = 6n - \frac{154n^2}{3} + \frac{8267n^3}{126} - \frac{146663n^4}{1151753n^4} + \frac{14143481n^5}{21027229n^5} + \frac{1344}{3360} - \frac{39916800}{24032441159n^6} + \frac{34594560}{1786716407701n^7} - \frac{697426329600}{153372726415967n^8} + \dots \\
 c_3 = \frac{146n^2}{2124n^3} - \frac{15}{2576596n^4} + \frac{210}{9257249n^5} - \frac{630}{3103882183n^6} + \frac{142560}{9696749750707n^7} - \frac{2402400}{96707303981543n^8} + \dots \\
 c_4 = \frac{3}{1207586n^4} - \frac{15}{9889618n^5} + \frac{105}{15800798789n^6} - \frac{4455}{3320773490077n^7} + \frac{2162160}{3730389142464631n^8} - \dots \\
 c_5 = \frac{315}{2221516n^5} - \frac{105}{164256182516n^6} + \frac{12474}{36404672059n^7} - \frac{270270}{131726046437189n^8} + \dots \\
 c_6 = \frac{63}{17067481924n^6} - \frac{155925}{7804602117964n^7} + \frac{2145}{1318332827886247n^8} - \dots \\
 c_7 = \frac{51975}{297742977176n^7} - \frac{675675}{81759539103832n^8} + \dots \\
 c_8 = \frac{96525}{82755885386882n^8} - \dots \\
 c_9 = \frac{2837835}{2837835} - \dots
 \end{cases} \tag{69}$$

$$\begin{cases}
 d_1 = 3n - \frac{89n^2}{12} + \frac{983n^3}{60} - \frac{669097n^4}{20160} + \frac{85205n^5}{1344} - \frac{4613096261n^6}{39916800} + \frac{7023747629n^7}{34594560} - \frac{241216793515063n^8}{697426329600} + \dots \\
 d_2 = \frac{73n^2}{6} - \frac{1214n^3}{225179n^4} + \frac{1229327n^4}{1173191n^5} - \frac{857341n^5}{134307704n^6} + \frac{1344}{190080} + \frac{39916800}{1029600} - \frac{34594560}{3321077760} + \dots \\
 d_3 = \frac{354n^3}{603793n^4} + \frac{15}{819668n^5} + \frac{210}{2298035959n^6} - \frac{630}{70583980717n^7} + \frac{1441440}{3821533260867121n^8} - \dots \\
 d_4 = \frac{1260}{1110758n^5} - \frac{105}{173808307n^6} + \frac{31185}{16232813323n^7} - \frac{135135}{137037324802363n^8} + \dots \\
 d_5 = \frac{315}{4266870481n^6} - \frac{2310}{32607070924n^7} + \frac{18018}{454957622901911n^8} - \dots \\
 d_6 = \frac{155925}{148871488588n^7} - \frac{45045}{12320936262697n^8} + \dots \\
 d_7 = \frac{675675}{41377942693441n^8} - \dots \\
 d_8 = \frac{22702680}{22702680} - \dots
 \end{cases} \tag{70}$$

$$\begin{cases}
 f_1 = \frac{3n}{2} - \frac{2n^2}{3} - \frac{47n^3}{48} + \frac{293n^4}{180} - \frac{241n^5}{1440} - \frac{72029n^6}{37800} + \frac{7021093n^7}{3225600} + \frac{5196481n^8}{50803200} - \dots \\
 f_2 = \frac{73n^2}{48} - \frac{19n^3}{1121n^4} - \frac{3427n^4}{1440} + \frac{3139n^5}{630} - \frac{81547n^6}{276480} - \frac{5357593n^7}{604800} + \frac{348016423n^8}{34836480} + \dots \\
 f_3 = \frac{177n^3}{80} - \frac{15}{603793n^4} - \frac{1440}{14843n^5} + \frac{1440}{12470017n^6} + \frac{630}{16018067n^7} - \frac{604800}{38515416901n^8} + \dots \\
 f_4 = \frac{603793n^4}{555379n^5} - \frac{420}{3803159n^6} - \frac{26880}{568876163n^7} + \frac{25920}{64225156139n^8} - \dots \\
 f_5 = \frac{80640}{4266870481n^6} - \frac{285120}{885241627n^7} + \frac{21288960}{3440458049657n^8} - \dots \\
 f_6 = \frac{319334400}{37217872147n^7} - \frac{28828800}{44517464099n^8} + \dots \\
 f_7 = \frac{1383782400}{41377942693441n^8} - \dots \\
 f_8 = \frac{743921418240}{743921418240} - \dots
 \end{cases} \tag{71}$$

$$\begin{cases}
 g_1 = n - \frac{29n^2}{12} + \frac{91n^3}{20} - \frac{160561n^4}{172103n^4} + \frac{272689n^5}{106159n^5} - \frac{891284321n^6}{659041567n^6} + \frac{18640929389n^7}{29059814447n^7} - \frac{788937772219n^8}{56935382676391n^8} + \dots \\
 g_2 = \frac{6}{122n^3} - \frac{15}{69337n^4} + \frac{3360}{107501n^5} - \frac{630}{77589203n^6} + \frac{1330560}{13448990773n^7} - \frac{21621600}{32131705046897n^8} + \dots \\
 g_3 = \frac{15}{49561n^4} - \frac{840}{181876n^5} + \frac{210}{153903661n^6} - \frac{31185}{12942105289n^7} + \frac{12972960}{214851406472257n^8} + \dots \\
 g_4 = \frac{1260}{69458n^5} - \frac{315}{1978379n^6} + \frac{31185}{1409842051n^7} - \frac{405405}{6583372516843n^8} + \dots \\
 g_5 = \frac{315}{212378941n^6} - \frac{462}{67083436804n^7} + \frac{30030}{11530411221457n^8} - \dots \\
 g_6 = \frac{155925}{6089027156n^7} - \frac{2027025}{25661491098559n^8} + \dots \\
 g_7 = \frac{675675}{1424729850961n^8} - \dots \\
 g_8 = \frac{22702680}{22702680} + \dots
 \end{cases} \tag{72}$$

$$\left\{ \begin{array}{l} k_1 = n - \frac{3n^3}{16} + \frac{15n^5}{256} + \frac{3n^7}{4096} + \dots \\ k_2 = -\frac{n^2}{4} - \frac{29n^6}{1024} - \frac{13n^8}{1024} - \dots \\ k_3 = \frac{n^3}{16} + \frac{n^5}{64} + \frac{31n^7}{2048} + \dots \\ k_4 = \frac{n^4}{64} - \frac{n^6}{128} - \frac{7n^8}{1024} - \dots \\ k_5 = \frac{n^5}{256} + \frac{3n^7}{1024} + \dots \\ k_6 = -\frac{n^6}{1024} - \frac{n^8}{1024} - \dots \\ k_7 = \frac{n^7}{4096} + \dots \\ k_8 = -\frac{n^8}{16384} - \dots \end{array} \right. \left\{ \begin{array}{l} l_1 = n - \frac{7n^3}{16} + \frac{71n^5}{256} - \frac{4201n^7}{36864} + \dots \\ l_2 = \frac{3n^2}{4} - \frac{5n^4}{6} + \frac{2317n^6}{3072} - \frac{8173n^8}{15360} + \dots \\ l_3 = \frac{13n^3}{16} - \frac{95n^5}{64} + \frac{18743n^7}{10240} - \dots \\ l_4 = \frac{197n^4}{192} - \frac{64}{5039n^6} + \frac{10240}{21233n^8} - \dots \\ l_5 = \frac{361n^5}{256} - \frac{42833n^7}{9216} + \dots \\ l_6 = \frac{10471n^6}{5120} - \frac{295949n^8}{35840} + \dots \\ l_7 = \frac{567409n^7}{184320} - \dots \\ l_8 = \frac{8191879n^8}{1720320} - \dots \end{array} \right. \tag{73}$$

$$\left\{ \begin{array}{l} m_1 = 4n - \frac{32n^2}{3} + \frac{124n^3}{5} - \frac{3296n^4}{63} + \frac{32476n^5}{315} - \frac{30081056n^6}{155925} + \frac{702328028n^7}{2027025} - \frac{25612953664n^8}{42567525} + \dots \\ m_2 = \frac{56n^2}{3} - \frac{1984n^3}{15} + \frac{65872n^4}{149984n^4} - \frac{105}{1085824n^5} - \frac{764096n^5}{1801378688n^6} + \frac{315}{85344488n^6} + \frac{10395}{110474417024n^7} - \frac{8775}{460933782976n^8} + \frac{29114859808n^8}{221278592n^7} + \frac{405405}{29114859808n^8} - \dots \\ m_3 = \frac{15}{1792n^3} - \frac{105}{149984n^4} + \frac{105}{1085824n^5} - \frac{31185}{1801378688n^6} + \frac{405405}{110474417024n^7} - \frac{405405}{460933782976n^8} + \dots \\ m_4 = \frac{273856n^4}{315} - \frac{931328n^5}{63} + \frac{4510583296n^6}{31185} - \frac{31185}{428596936192n^7} + \frac{405405}{7739219530112n^8} - \frac{405405}{1216215} - \dots \\ m_5 = \frac{2137088n^5}{315} - \frac{57822208n^6}{385} + \frac{31185}{27867235328n^7} - \frac{405405}{2267235680768n^8} + \frac{1216215}{135135} + \dots \\ m_6 = \frac{1232232448n^6}{22275} - \frac{3063276371968n^7}{2027025} + \frac{15015}{6541987361792n^8} - \dots \\ m_7 = \frac{314093993984n^7}{675675} - \frac{18390588870656n^8}{1216215} + \dots \\ m_8 = \frac{11331532414976n^8}{2837835} - \dots \end{array} \right. \tag{74}$$

References

Bermejo-Solera M, Otero J (2009) Simple and highly accurate formulas for the computation of transverse Mercator coordinates from longitude and isometric latitude. *J Geodesy* 83(1):1–12. <https://doi.org/10.1007/s00190-008-0224-y>

Bowman F (1961) *Introduction to elliptic functions: with applications*. Dover Publications, New York

Byrd PF, Friedman MD (1971) *Handbook of elliptic integrals for engineers and physicists*, 2nd edn. Springer-Verlag, Berlin

Cuyt AA, Petersen V, Verdonk B, Waadeland H, Jones WB (2008) *Handbook of continued fractions for special functions*. Springer, Berlin

Dorrer E (2003) From elliptic arc length to Gauss-Krüger coordinates by analytical continuation. In: Grafarend E, Krumm FW, Schwarze VS (eds) *Geodesy-the challenge of the 3rd millennium*. Springer, Berlin, pp 293–298

Dozier J (1980) Improved algorithm for calculation of UTM and geodetic coordinates. Technical report, NESS 81. NOAA. <http://fiest.a.bren.ucsb.edu/~dozier/Pubs/DozierUTM1980.pdf>

Engsager K, Poder K (2007) A highly accurate world wide algorithm for the transverse Mercator mapping (almost). In: *Proceedings of XXIII international cartographic conference (ICC2007)*, pp 4–10

Enríquez C (2004) Accuracy of the coefficient expansion of the transverse Mercator projection. *Int J Geogr Inf Sci* 18(6):559–576. <https://doi.org/10.1080/13658810410001701996>

Grafarend EW, Syffus R (1998) The solution of the Korn-Lichtenstein equations of conformal mapping: the direct generation of ellipsoidal Gauss-Krüger conformal coordinates or the transverse

Mercator projection. *J Geodesy* 72(5):282–293. <https://doi.org/10.1007/s001900050167>

Grafarend EW, You RJ, Syffus R (2014) *Map projections*. Springer, Berlin

Hazewinkel M (2012) *Isothermal coordinates*, encyclopedia of mathematics. Springer, Berlin

Hotine M (1946) The orthomorphic projection of the spheroid. *Empire Survey Review* 9(63):25–35. <https://doi.org/10.1179/sre.1946.8.62.300>

Karney CFF (2011) Transverse Mercator with an accuracy of a few nanometers. *J Geodesy* 85(8):475–485. <https://doi.org/10.1007/s00190-011-0445-3>

König R, Weise KH (1951) *Mathematische Grundlagen der Höheren Geodäsie und Kartographie: Erster Band: Das Erdsphäroid und Seine Konformen Abbildungen*, vol I. Springer, Berlin

Krüger L (1912) *Konforme Abbildung des Erdellipsoids in der Ebene*, vol 52. BG Teubner, Berlin

Lambert JH (1972) *Anmerkungen und Zusätze zur Entwerfung der Land-und Himmelscharten*. No. 54 in *Klassiker ex. Wiss.*, Engelmann, Leipzig (1894), http://books.google.com/books?id=o_s_MR3NUD4C, translated into English by W. R. Tobler as *Notes and Comments on the Composition of Terrestrial and Celestial Maps*, University of Michigan (1972)

Lee LP (1962) The transverse Mercator projection of the entire spheroid. *Empire Surv Rev* 16(123):208–217. <https://doi.org/10.1179/sre.1962.16.123.208>

Lee LP (1963) Scale and convergence in the transverse Mercator projection of the entire spheroid. *Surv Rev* 17(127):49–51. <https://doi.org/10.1179/sre.1963.17.127.49>

- Lee LP (1976) Conformal projections based on Jacobian elliptic functions. *Cartogr Int J Geogr Inf Geovis* 13(1):67–101. <https://doi.org/10.3138/X687-1574-4325-WM62>
- Ludwig K (1943) Die der transversalen Mercatorkarte der Kugel entsprechende Abbildung des Rotationsellipsoids. *Journal für die reine und angewandte Mathematik* 185:193–230
- McConnell S (2013) The Riemann mapping theorem <http://math.uchicago.edu/~may/REU2013/REUPapers/McConnell.pdf>
- Munkres JR (2000) *Topology*, 2nd edn. PHI learning private limited,
- Olver FWJ, Lozier DW, Boisvert RF, Clark CW (2010) *NIST handbook of mathematical functions*. Cambridge University Press, Cambridge
- Poder K, Engsager K (1998) *Some conformal mappings and transformations for geodesy and topographic cartography*. Kort & Matrikelstyrelsen, København
- PROJ contributors (2020) PROJ coordinate transformation software library. Open Source Geospatial Foundation, <https://proj.org/>
- Redfearn JCB (1948) Transverse Mercator formulae. *Empire. Surv Rev* 9(69):318–322. <https://doi.org/10.1179/sre.1948.9.69.318>
- Thomas PD (1952) *Conformal projections in geodesy and cartography*. Special Publication 251. US Coast and Geodetic Survey., http://docs.lib.noaa.gov/rescue/cgs/_specpubs/QB275U35no2511952.pdf
- Thompson EH (1975) A note on conformal map projections. *Surv Rev* 23(175):17–28. <https://doi.org/10.1179/sre.1975.23.175.17>
- Turiño CE (2008) Gauss Krüger projection for areas of wide longitudinal extent. *Int J Geogr Inf Sci* 22(6):703–719. <https://doi.org/10.1080/13658810701602286>
- Wolfram S (2017) *An elementary introduction to the Wolfram language*, 2nd edn. Wolfram Media, Peru